

Damping of large-amplitude solitary waves

Roger Grimshaw¹⁾, Efim Pelinovsky²⁾ and Tatiana Talipova²⁾

¹⁾Department of Mathematical Sciences,
Loughborough University, Loughborough, UK

²⁾Laboratory of Hydrophysics and Nonlinear Acoustics,
Institute of Applied Physics, Nizhny Novgorod, Russia

March 26, 2002

1 Introduction

Soliton damping in weakly dissipative media has been studied for several decades, usually using the asymptotic theory of the slowly-varying solitary wave solution of the Korteweg-de Vries (KdV) equation. Damping then occurs according to the energy balance equation, and a shelf is generated behind the soliton. Various examples of this process have been given by Ott & Sudan (1970) Pelinovsky (1971), Karpman & Maslov (1977), Grimshaw (1981), Grimshaw (1983), Newell (1985), and Smyth (1988).

However, for many cases in nonlinear wave dynamics, such as for internal solitary waves in the ocean and atmosphere, the nonlinearity is not so weak as is implied by the KdV equation. In the next order of the perturbation theory, a higher-order KdV equation can be obtained, which in general includes cubic nonlinearity, fifth-order linear dispersion, and nonlinear dispersion. The contribution of the various high-order terms depends on the parameters of the model (e.g. density stratification and shear flow), and sometimes several of them may be more important. For instance for internal waves in a two-layer fluid the quadratic nonlinear term vanishes when the pycnocline lies in the middle of fluid (in the Boussinesq approximation) and then it is the cubic nonlinear term which is the most important, so that the higher-order equation reduces to the modified KdV equation. In the absence of any damping term, this last equation is fully integrable, as is of course the KdV equation. For certain environmental conditions when the quadratic nonlinear term is small, the cubic nonlinear term becomes the major from the high-order terms and it should be taken into account together with the quadratic nonlinear term. The corresponding equation

$$\frac{\partial u}{\partial t} + \alpha u \frac{\partial u}{\partial x} + \beta u^2 \frac{\partial u}{\partial x} + \frac{\partial^3 u}{\partial x^3} = 0 \quad (1)$$

is known as the extended Korteweg-de Vries (eKdV) equation, or the Gardner equation. This equation has been used as a model of strongly nonlinear internal waves in the ocean (Holloway et al, 2001). The coefficient β of the cubic

nonlinear term may take either sign depending on the fluid stratification. For the classical two-layer model it is always negative, but for certain three-layer models, it may be negative, or positive, or zero (Grimshaw et al, 1997). The solutions of the eKdV equation describe various kinds of nonlinear waves (solitons, breathers, dissipationless shock waves) for the various signs of the coefficients of the quadratic and cubic nonlinear terms. A knowledge of possible wave regimes is very important for an understanding of nonlinear wave dynamics in the ocean and atmosphere. Further equation (1) is integrable, but unlike the KdV equation, the number of explicitly solved problems is small. In particular, soliton interaction has been investigated by Slunyaev & Pelinovsky (1999) and Slunyaev (2001) for both signs of the cubic nonlinear term. Instability of the algebraic solitons in the eKdV equation has been studied by Pelinovsky & Grimshaw (1997); any disturbance leads to the transformation of the algebraic soliton to a "normal" soliton, or to a breather. Interesting example of the soliton transformation when the quadratic nonlinear term changes its sign (this situation is realised for internal waves in the coastal zone with an inclined pycnocline) was given by Grimshaw et al (1999). The influence of all high-order terms on the soliton dynamics was investigated numerically by Marchant & Smyth (1990, 1996).

Our purpose here is to consider the eKdV equation supplemented with a damping term, so that (1) is replaced by written as

$$\frac{\partial u}{\partial t} + \alpha u \frac{\partial u}{\partial x} + \beta u^2 \frac{\partial u}{\partial x} + \frac{\partial^3 u}{\partial x^3} + \nu T\{u\} = 0, \quad (2)$$

where the term $T\{u\}$ is in general a nonlinear integro-differential operator described wave dissipation, and ν is a small parameter. In the linear case, the operator T can be presented as

$$T\{u\} = \frac{1}{2\pi} \int_{-\infty}^{\infty} g(k) \exp(ikx) u(k) dk, \quad (3)$$

where $u(k)$ is the spectrum of the wave field, and $g(k)$ is the linear decrement. For instance, when $g(k) = k^2$, the operator $T = -\partial^2 u / \partial x^2$, and (2) can be called the eKdV-Burgers equation; we call this case "linear viscosity". When the dissipation is principally due to a laminar boundary layer at a rigid boundary (bottom of the ocean), $g(k) = (-ik)^{1/2}$, and the dissipative term in (2) is an integro-differential operator (Grimshaw, 1981; Smyth, 1988; Craig, 1991). A turbulent boundary layer is often parametrised either by linear friction, $T = u$ (Brink, 1988), or by a quadratic term (Chezy friction), $T = |u|u$ (Holloway et al, 2001).

If the dissipation, ν is small, damping of the solitary wave can be studied with the use of asymptotic methods developed for perturbed solitons, see, for instance, Karpman & Maslov (1977), Newell (1985), and Grimshaw & Mitsudera (1993). In the first approximation, the variation of the solitary wave amplitude

can be found from the energy balance equation obtained from (2)

$$\frac{dP}{dt} = -\nu \int_{-\infty}^{\infty} uT\{u\}du, \quad (4)$$

$$\text{where } P = \int_{-\infty}^{\infty} \frac{1}{2}u^2dx, \quad (5)$$

is the momentum (energy), by simply substituting the expression for a solitary wave directly into (4). This procedure is standard now. For weak-amplitude solitary waves ($\beta = 0$), all known results can be obtained in this manner from (5). Our aim is to obtain some new nontrivial results for large-amplitude solitary waves.

2 Damping of “thick” solitary waves

When the coefficient β of the cubic nonlinear term is negative, the solitary wave solution of the eKdV equation (1) may be presented explicitly,

$$u(x, t) = \frac{\alpha}{\beta} \frac{B^2 - 1}{1 + B \cosh[\gamma(x - \gamma^2 t)]}, \quad \gamma^2 = \frac{\alpha^2}{6\beta}(B^2 - 1), \quad a = \frac{\alpha}{\beta}(B - 1), \quad (6)$$

where γ is a free parameter, characterising the inverse width of the solitary wave, a is the wave amplitude (peak value), and $0 < B < 1$. The solitary wave has positive polarity, that is, $a\alpha > 0$. Its shape for $\alpha = 1, \beta = 1$ is shown in Figure 1. At small wave amplitudes ($\gamma \rightarrow 0$ or $B \rightarrow 1$) the solitary wave (6) transforms into the KdV soliton

$$u = a \operatorname{sech}^2 \left[\sqrt{\frac{\alpha a}{12}} \left(x - \frac{\alpha a}{3} t \right) \right]. \quad (7)$$

As $B \rightarrow 0$, the wave amplitude increases and approaches the limiting value,

$$a_{lim} = \frac{\alpha}{|\beta|}, \quad (8)$$

while the width of the solitary wave increases to infinity; it becomes the so-called “thick” soliton, see Figure 1. The “thick” soliton can be presented in the form of a kink-antikink combination

$$u(x, t) =, \frac{a_{lim}}{2} [\tanh Z_+ - \tanh Z_-], \quad Z_{\pm} = \frac{\alpha}{\sqrt{24|\beta|}} \left(x - \frac{\alpha^2}{6\beta} t \pm L/2 \right), \quad (9)$$

where L is the distance between the kink and antikink, and is the effective width of the solitary wave ($L = \sqrt{24|\beta|} |\ln B|/\alpha$). The two almost independent parts of the solitary wave, namely the “high-wavenumber” kink - antikink pair, and

the almost constant top (“table-hill”) can have different responses to dissipative processes.

First, let us consider, the linear friction case, $T = u$, when the damping is independent of wavenumber. In this case the energy balance equation (4) can be integrated to give,

$$P(t) = P_0 \exp(-2\nu t), \quad (10)$$

where P_0 is the initial soliton momentum. The relation between the momentum, P and amplitude, a is given by (Grimshaw et al, 1999),

$$P = \frac{\alpha\sqrt{6|\beta|}}{\beta^2} \left[2 \tanh^{-1} \sqrt{\frac{a/a_{lim}}{2 - a/a_{lim}}} - \sqrt{\frac{a}{a_{lim}} \left(2 - \frac{a}{a_{lim}} \right)} \right], \quad (11)$$

For the “thick” soliton $P \sim a_{lim}^2 L$. It means that the distance between the kinks decreases as

$$L(t) = L_0 \exp(-2\nu t) \quad (12)$$

due to the damping. When the kinks are close each to other, the “thick” soliton transforms into the “normal” (KdV-like) soliton, and then its amplitude will decrease tending to the dependence

$$a \sim \exp\left(-\frac{4\nu t}{3}\right), \quad (13)$$

known for the damping of the KdV soliton.

Also, the equation for conservation of mass obtained from equation (2) can be integrated for this case of linear friction to give,

$$M(t) = \int_{-\infty}^{\infty} u(x, t) dx = M_0 \exp(-\nu t), \quad (14)$$

Using (6) the soliton mass can be calculated

$$M_s = 4\sqrt{\frac{6}{|\beta|}} \tanh^{-1} \sqrt{\frac{a/a_{lim}}{2 - a/a_{lim}}}. \quad (15)$$

It is easily to show that the soliton mass differs from (14). It means that a tail will form behind the soliton and its mass (normalised by M_0) is displayed in Figure 2. In particular, in the weak-amplitude limit (KdV limit) $M_s \sim \exp(-2\nu t/3)$ which is decaying more slowly than the total mass (14), and this means that the tail mass is negative, and is described by

$$M_t = M_0 (\exp(-\nu t) - \exp(-2\nu t/3)). \quad (16)$$

On the other hand, the “thick” soliton mass is $M_{sol} \sim a_{lim} L \sim \exp(-2\nu t)$, and it is damping faster than the total mass (14). Thus, a positive tail should

form behind the “thick” soliton. The transition value a_{tr} of the initial wave amplitude, below which the tail mass is negative, can be found from the transcendental equation

$$\frac{M_0}{P_0} = 2 \frac{dM_0}{dP_0}, \quad (17)$$

and it is $a_{tr}/a_{lim} \simeq 0.61$.

The results of this perturbation theory for the soliton damping are confirmed by numerical simulations in the framework of (2) for $\alpha = 1$, $\beta = -1$ and $\nu = 10^{-4}$. The solitary wave keeps its “soliton” form and its amplitude is described by the theoretical formula very well, but we will not display this case. The polarity of the wave tail coincides with theory also (see Figure 2). The condition of the applicability of this adiabatic theory is the weakness of the last dissipative term in (2) in comparison with the nonlinear and dispersive terms. For the “thick” soliton it reduces to

$$\nu L^3 \ll 1. \quad (18)$$

As the distance between the distance between the kinks increases, (or as the friction coefficient increases), the coherence of the solitary wave breaks and the kinks become more independent. As a result, the linear friction acts on the “table” crest independently from the kinks resulting in its damping as $\exp(-\nu t)$. Thus a wide impulse with an amplitude just less than the limiting one has no quasi-steady-state form, and will evolve mainly due to the joint action of the nonlinearity, dispersion and dissipation. The forward (right) kink is more stable due to the opposite action of nonlinearity and dispersion. The backward (left) kink (antikink) will smooth because nonlinearity and dispersion act in the same direction. As a result, the wave profile becomes more asymmetric like a “quasi-shock” wave. This process is illustrated in Figure 3 (see the profile at time 200) where the results of numerical simulation of equation (2) for $\nu = 0.001$ are presented. The upper part of the wave forms into a soliton-like wave. The lower part of the wave is the positive tail, and tends to have a triangular form (see times 300 - 400). As the wave amplitude decreases, the generation of the tail is reduced (for the adiabatic stage the critical value of the amplitude is $0.61a_{lim}$), and the positive wave tail transforms into an isolated impulse (times 800 and greater). Due to its small amplitude it not moves quite slowly, (see the upper part of Figure 3 where contours of the wave field in the $x - t$ plane are given). The leading solitary wave and the secondary impulse separate in space. When the friction coefficient is increased to $\nu = 0.005$, the tail is more energetic (see Figure 4) and it attempts to split into two impulses (it is more visible in the upper part of Figure 4). But the wave damping is also increased, and the primary and secondary waves cannot separate significantly in space. When the friction is larger still ($\nu = 0.05$), an initial soliton damps rapidly as a linear wave, and there is no formation of the secondary waves (see Figure 5).

Thus, the main feature of the damping of a “thick” solitary wave due to linear friction is the formation of the secondary impulses, a process apparently not previously reported in the literature. For weak-amplitude solitons (KdV-limit) the tail is negative and it damps as the oscillatory wave packet.

Second, consider the linear viscosity case, when $T = -\partial^2 u / \partial^2 x$, and equation (2) transforms to the extended KdV-Burgers equation. In this case the momentum balance equation has the form

$$\frac{dP}{dt} = -\nu D = -\nu \int_{-\infty}^{\infty} \left(\frac{\partial u}{\partial x} \right)^2 dx. \quad (19)$$

The integral D is given by

$$D = \frac{\alpha^3}{3\beta^2 \sqrt{6|\beta|}} \tilde{D}, \quad (20)$$

$$\tilde{D} = \left[1 + 2 \left(1 - \frac{a}{a_{lim}} \right)^2 \right] \sqrt{\left(\frac{a}{a_{lim}} \right) \left(2 - \frac{a}{a_{lim}} \right)} - 6 \left(1 - \frac{a}{a_{lim}} \right)^3 \operatorname{atanh} \sqrt{\frac{a/a_{lim}}{2 - a/a_{lim}}}.$$

In particular, for the weak-amplitude KdV solitons equation (19) gives

$$a(t) = \frac{a_0}{1 + 4\alpha a_0 \nu t / 45}. \quad (21)$$

For the “thick” soliton, the energy dissipation is concentrated entirely in the kinks, and the function $\tilde{D} \rightarrow 1$ so that D takes the constant value,

$$D_{lim} = \frac{\alpha^3}{3\beta^2 \sqrt{6|\beta|}}. \quad (22)$$

As a result, the momentum of the “thick” solitary wave (or the distance between the kinks) damps linearly

$$P(t) = P_0 - \nu D_{lim} t. \quad (23)$$

Also it is easily shown that the total mass, M is conserved, but the soliton mass, M_s is decreases. As a result, the tail generated behind the solitary wave has positive mass for any initial amplitude.

For the validity of the adiabatic theory for weakly-damped solitary waves (with a rigid relation between the kinks through the “table” crest) it is necessary to have a very small dissipative coefficient

$$\nu L \ll 1. \quad (24)$$

The adiabatic stage of the solitary wave damping in this case is quite similar to the adiabatic stage with the linear friction damping; the solitary wave keeps its form, and a very small tail of positive polarity is generated (in previous case it can have different polarity depending on the amplitude). This adiabatic stage will be not discussed here in any further detail.

The non-adiabatic stage of soliton damping was studied numerically, and these results are presented in Figure 5 for $\alpha = 1$, $\beta = -1$ and $\nu = 0.05$. The tail forms on the back-face of the solitary wave (see the times 400 and 800). With decreasing of the solitary wave amplitude, the tail becomes weaker and eventually separates from the primary wave (see times 1200 and 2400). It has very large length, and the further evolution is controlled mainly by the nonlinearity, so that it transforms into a shock wave. The primary wave damps and its speed decreases. The “shock-wave” tail overtakes the small solitary wave and absorbs it (see times 6000 and 20000). This overtaking at the time around 10000 is clearly seen in the upper part of Figure 5 in the $x - t$ plot. In fact, this process of soliton damping by the viscosity in this last stage (when the wave amplitude is weak) is similar to the theory for soliton damping in the KdV model (Grimshaw, 1983).

With the viscosity is increased ($\nu = 0.5$) the friction term dominates over the dispersive term, and the solitary wave transforms to a shock wave, as it should be the case in the Burgers equation (Figure 6). The influence of the cubic nonlinearity leads here to a different shape For the back-face of the wave. In the Burgers model the back-face is described by the self-similar solution

$$\alpha u(x, t) = \frac{x}{t}, \quad (25)$$

which is the same as when the viscosity is zero, but here in the extended Burgers model the self-similar solution is

$$\alpha u + \beta u^2 = \frac{x}{t}, \quad (26)$$

and this difference is important for large amplitudes, see Figure 6 for time 600. In the final stage, when the wave amplitude is weak, the back-face becomes linear, and the wave transforms into the triangular shock, according to predictions in the framework of the Burgers equation.

3 Soliton transformation into a wave packet

When the coefficient β of the cubic nonlinear term is positive, there are two families of solitary wave solutions of equation (1). They are also described by (6) but with $B^2 > 1$. The positive solitons ($1 < B < \infty$) with a weak amplitude are the solitons of the KdV equation, while those of large amplitude are solitons of the modified KdV equation. Overall, the damping of these solitons is similar to that for the dynamics KdV solitons and will not be discussed here. The other

family of solitary waves has negative polarity and are realised for negative B ($-\infty < B < -1$). For large amplitude ($B \rightarrow -\infty$) this wave is also the soliton of the modified KdV equation, but its amplitude now is negative. The amplitudes (in modulus) of these negative solitons should be greater than critical value,

$$a_{cr} = -\frac{2\alpha}{\beta}. \quad (27)$$

As the amplitude tends to the critical value ($B \rightarrow -1$), this wave becomes the standing algebraic soliton

$$u(x) = \frac{a_{cr}}{1 + \alpha^2 x^2 / 6\beta}. \quad (28)$$

The shape of this last family of the solitary waves (for $\alpha = -1$, $\beta = 1$) is shown in Figure 7 (normalised by a_{cr}). In the “gap” area, there are no steady-state solutions, but instead breather solutions exist and solitons can be transformed into breathers (Pelinovsky & Grivshaw, 1997; Grimshaw et al, 1999). The same effect is expected here due to dissipative effects.

The adiabatic stage of the solitary wave transformation can again be studied using the momentum balance equation (10) or (19) depending on the form of the dissipation. The momentum of the solitary wave is here expressed by

$$P = \frac{2\alpha}{\beta} \sqrt{\frac{6}{\beta}} \left[\sqrt{\frac{a}{a_{cr}} \left(\frac{a}{a_{cr}} - 1 \right)} + a \tan \sqrt{\frac{a/a_{cr}}{a/a_{cr} - 1}} \right], \quad (29)$$

(compare (11)). This function is a monotonic function of the soliton amplitude. For large-amplitude solitary waves it coincides with the momentum of the modified KdV soliton

$$P = |a| \sqrt{\frac{6}{\beta}}, \quad (30)$$

and for the algebraic soliton the momentum is a constant,

$$P_{cr} = \frac{\pi\alpha}{\beta^2} \sqrt{6\beta}. \quad (31)$$

The solitary waves of large amplitude damp as solitons of the modified KdV equation, exponentially for linear friction

$$a(t) = a_0 \exp(-2\nu t), \quad (32)$$

and as

$$a(t) = \frac{a_0}{\sqrt{1 + 2\nu\beta a_0^2 t/9}} \quad (33)$$

for linear viscosity. Due to dissipation the solitary wave momentum approaches the fixed non-zero value (31), and cannot decrease further. Because there is no

soliton solution with momentum less than P_{cr} , solitary wave will destruct and transform into a wave packet. This stage can not be described in the framework of the adiabatic perturbation method.

Numerical simulations of equation(2) were performed to study the generation of wave packets from the initial solitary wave for $\alpha = -1$, $\beta = 1$, and various dissipative coefficients ν . The initial amplitude, $a_0 = 2.5$ in all runs is close to the critical value, $a_{cr} = 2$. First, let us consider the linear viscosity case. The results of numerical simulations of soliton damping due to a small linear viscosity ($\nu = 0.001$) are shown in Figure 8, where the temporal evolution of the wave field is shown in an $x - t$ plot (upper part), and the spatial Fourier spectrum is shown in a $k - t$ plot (lower part). In the $x - t$ plot the wave trajectory at first corresponds to the soliton trajectory, inclined downwards (with a speed exceeded the linear long-wave phase speed, 0 here), and then to a wave packet trajectory inclined upwards (with speed less than the linear long-wave phase speed). The solitary wave transforms into a breather, which is close to a pair of two oscillating solitons (the colour of the soliton trajectory varies periodically). For very large times, the breather transforms into a wave packet, due to damping (middle part of Figure 8). Also a weak positive impulse is visible in Figure 8 at this time, which propagates approximately with the linear long-wave phase speed and is located in front of the wave packet. The Fourier spectrum of the wave packet for large times has two components: $k = 0.5$ (oscillatory part) and $k = 0$. The zero component can be explained by mass conservation obtained from (2) with linear viscosity.

With increasing of the viscosity ($\nu = 0.015$) the process of the breather transformation into a wave group, and a low-wavenumber impulse are more clearly seen. Figure 9 shows the evolution of the wave field (upper part) and its spectrum (lower part). The wave packet now is wider and is closer to the wave packet with a steady-state envelope like the solitary waves in the nonlinear Schrodinger equation. The equivalence between weak amplitude breathers in the extended KdV equation and envelope solitons in the nonlinear Schrodinger equation was established by Grimshaw et al (2001). For large times the wave packet damps and only the low-wavenumber impulse propagates (it is clearly visible in the spectral plane). The dynamics of this impulse for long times is shown in Figure 10. The impulse has the triangular form corresponding to a shock wave (because $\alpha < 0$ the back-face is steeper than the forward face).

The results of numerical simulations for soliton damping by the linear friction are similar to those described above: the initial solitary wave after approaching to the critical value transforms into a damped breather, and an impulse located in front of the wave group. The dynamics of the impulse (zero component) in the case of the linear friction differs from that considered above. The impulse is more symmetric and does not transform into a shock wave. Instead, the friction acts on all spectral components equally and the impulse hence damps at the same rate as the wave packet. As a result, the wave packet remains more energetic than the impulse, and this is clear seen in Figure 11.

4 Conclusion

The eKdV equation (1) is a model for the description of large-amplitude solitary waves in density-stratified shear flows. Weak dissipation, always present in the medium, leads to the damping of solitary waves. This process may differ from that known for the KdV model. The results described here characterize the main features of the damping of large-amplitude solitary waves, in comparison with that for to KdV solitons.

When the coefficient of the cubic nonlinear term is negative, there is one family of solitary waves, ranging from the soliton of the KdV equation for the weak amplitudes, into the “thick” solitary wave (kink-antikink system) when the amplitude approaches to the limiting value a_{lim} (see (8)). In the case of linear friction the damping of a large-amplitude solitary wave is accompanied by the formation of a tail of the same polarity as the solitary wave, while the decay of weak-amplitude waves is accompanied by the formation of a tail of the opposite polarity. For a very weak dissipation, when asymptotic perturbation methods can be used, the transition value of the soliton amplitude distinguishing these cases is $0.61a_{lim}$. When the dissipation is not too small, the tail formed behind the large-amplitude solitary wave has enough mass and momentum to transform into a group of secondary waves. The primary and secondary waves separate in space.

In the case of the linear viscosity (high-wavenumber damping) the polarity of the tail behind of the solitary wave is the same as the soliton polarity for all amplitudes. It has a relatively large length and evolves mainly as a shock wave. The solitary wave damps more rapidly and its speed becomes less than the tail speed. As a result, the shock-wave tail overtakes the small solitary wave and absorbs it. Also the form of the back-face of the damped large-amplitude solitary wave differs from the straight line characterised by the KdV-Burgers solution.

When the coefficient of the cubic nonlinear term is positive, there are two families of the solitary waves. One of them having a polarity opposite to the sign of the coefficient of the quadratic nonlinear term, has the lower limit in amplitude, and so for small amplitudes, the soliton solutions conjugate with the breather solutions. The damping of these solitons has very interesting features. For large amplitudes the solitary wave damps as the soliton of the modified KdV equation. In finite time the soliton amplitude approaches to the critical value, and the solitary wave transforms into a breather which for longer times transforms to a weak-amplitude breather (wave packet with soliton envelope) and a low-wavenumber isolated impulse. The dynamics of this impulse depends on the character of the dissipation. For the case of the linear viscosity, when the total wave mass is conserved, the impulse transforms into a triangular shock wave, and this is the final stage of the solitary wave damping. For the case of the linear friction this impulse always has less amplitude than the wave packet (breather) due to the decrease of the total mass.

Acknowledgement. This work was carried out with partial support from INTAS (99-1068 and 01-2156) for EP, and INTAS (01-25) and RFBR (00-05-64223) for TT.

References

- [1] **Brink K.H.** On the effect of bottom friction on internal waves. *Continental Shelf Research*, 1988, 8, 4, 397 - 403.
- [2] **Craig P.** Incorporation of damping into internal wave models. *Continental Shelf Research*, 1991, v. 11, 563 - 577.
- [3] **Grimshaw, R.** Evolution equations for long, nonlinear internal waves in stratified shear flows. *Studies Applied Math.*, 1981, v. 65, 159 - 188.
- [4] **Grimshaw, R.** Solitary waves in slowly varying environments: long nonlinear waves. In: *Nonlinear Waves* (Ed. L. Debnath). Cambridge Univ. Press. 1983, 44 - 67.
- [5] **Grimshaw, R., Pelinovsky, E. and Talipova, T.** The modified Korteweg-de Vries equation in the theory of the large-amplitude internal waves. *Nonlinear Processes in Geophysics*, 1997, v. 4, 237 - 250.
- [6] **Grimshaw, R., Pelinovsky, E., and Talipova, T.** Solitary wave transformation in a medium with sign-variable quadratic nonlinearity and cubic nonlinearity. *Physica D*, 1999, v. 132, 40 - 62.
- [7] **Grimshaw, R., Pelinovsky, E., and Talipova, T.** Wave group dynamics in weakly nonlinear long-wave models. *Physica D*, 2001, v. 159, 35 - 57..
- [8] **Holloway, P., Pelinovsky, E., and Talipova, T.** Internal tide transformation and oceanic internal solitary waves. Chapter 2 in the book: *Environmental Stratified Flows* (Ed. R. Grimshaw). Kluwer Acad. Publ. 2001, 29-60.
- [9] **Karpman, V.I., and Maslov, E.M.** Perturbation theory for solitons. *JETP*. 1977, v. 73, 537 - 559.
- [10] **Marchant, T.R. and Smyth, N.F.** The extended Korteweg-de Vries equation and the resonant flow over topography. *J. Fluid Mech.* 1990, v. 221, 263 - 288.
- [11] **Marchant, T.R. and Smyth, N.F.** Soliton interaction for the extended Korteweg - de Vries equation. *J. Appl. Math.*, 1996, v. 56, 157 - 176.
- [12] **Newell, A.** Solitons in mathematics and physics, SIAM Philadelphia, 1985.
- [13] **Ott, E., and Sudan, R.N.** Damping of solitary waves, *Phys. Fluids*, 1970, v. 13, 1432 - 1434.

- [14] **Pelinovsky, D., and Grimshaw, R.** Structural transformation of eigenvalues for a perturbed algebraic soliton potential. *Phys. Lett.*, 1997, v. A229, 165 - 172
- [15] **Pelinovsky, E.N.** On the Absorption of Nonlinear Waves in Dispersive Media. *J. Appl. Mech. Tech. Phys.*, 1971, N. 2, 68 - 71.
- [16] **Slyunyaev, A.V.** Dynamics of localized waves with large amplitude in a weakly dispersive medium with a quadratic and positive cubic nonlinearity. *JETP*, 2001, v. 119, 606-612.
- [17] **Slyunyaev, A., Pelinovskii, E.** Dynamics of large-amplitude solitons. *JETP*, 1999, v. 89, N. 1, 173 - 181.
- [18] **Smyth, N.F.** Dissipative effects on the resonant flow of a stratified fluid over topography, *J. Fluid Mech.*, 1988, v. 192, 287 - 312.

Figure Captions

Figure 1. The shape of solitary wave solutions of equation (1) when the coefficient β of the cubic nonlinear term is negative.

Figure 2. The tail mass as a function of time in the adiabatic approximation, for the linear friction case, when $\beta < 0$.

Figure 3. Evolution of the solitary wave for the linear friction case, $\nu = 0.001$, when $\beta < 0$.

Figure 4. The same as in Figure 3, but for $\nu = 0.005$

Figure 5. Evolution of the solitary wave for the linear viscosity case, $\nu = 0.05$, when $\beta < 0$.

Figure 6. The same as in Figure 5, but for $\nu = 0.5$

Figure 7. The shape of solitary wave solutions of equation (1) when the coefficient β of the cubic nonlinear term is positive.

Figure 8. Transformation of a solitary wave into a wave packet for the linear viscosity case, $\nu = 0.001$, when $\beta > 0$.

Figure 9. The same as in Figure 8, but for $\nu = 0.015$.

Figure 10. Long term evolution of the wave field after soliton damping, for the linear viscosity case, when $\beta > 0$.

Figure 11. Transformation of a solitary wave into a breather for the linear friction case, when $\beta > 0$.

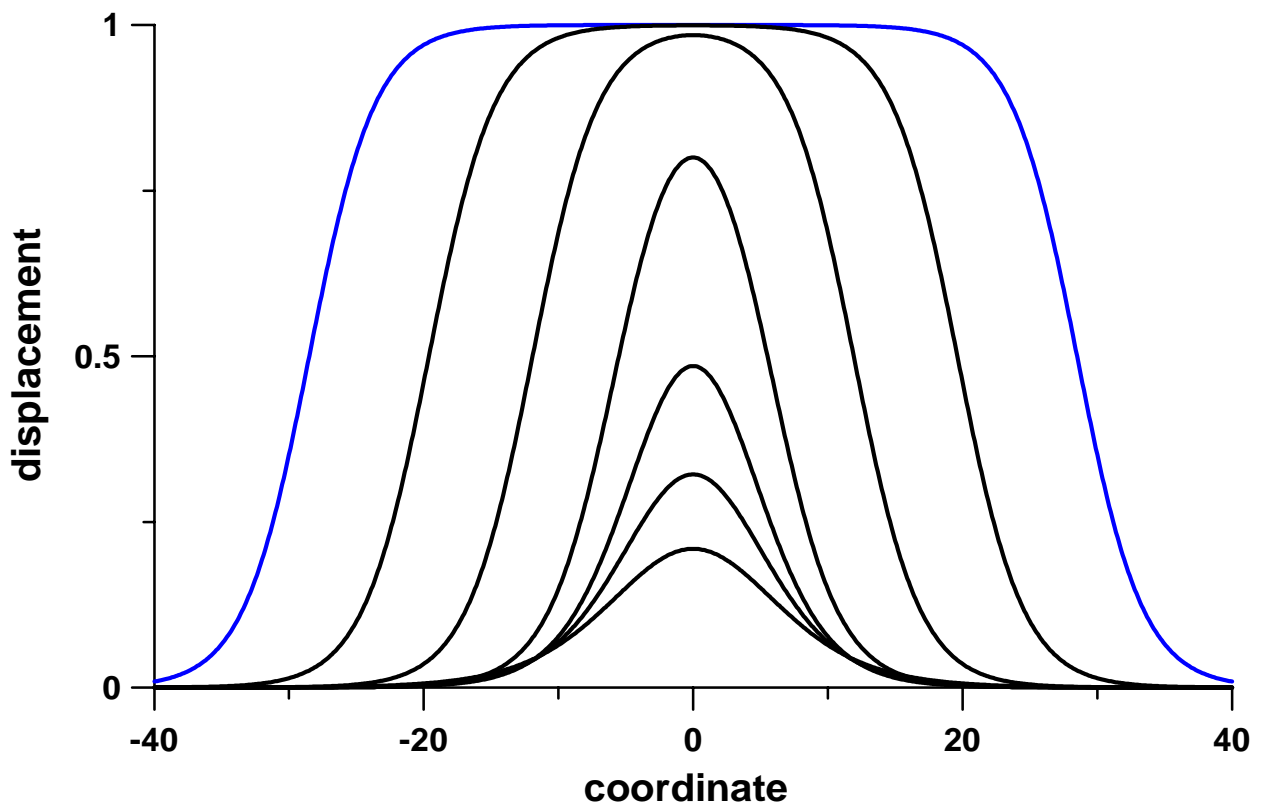


Figure 1. The shape of solitary wave solutions of equation (1) when the coefficient β of the cubic nonlinear term is negative

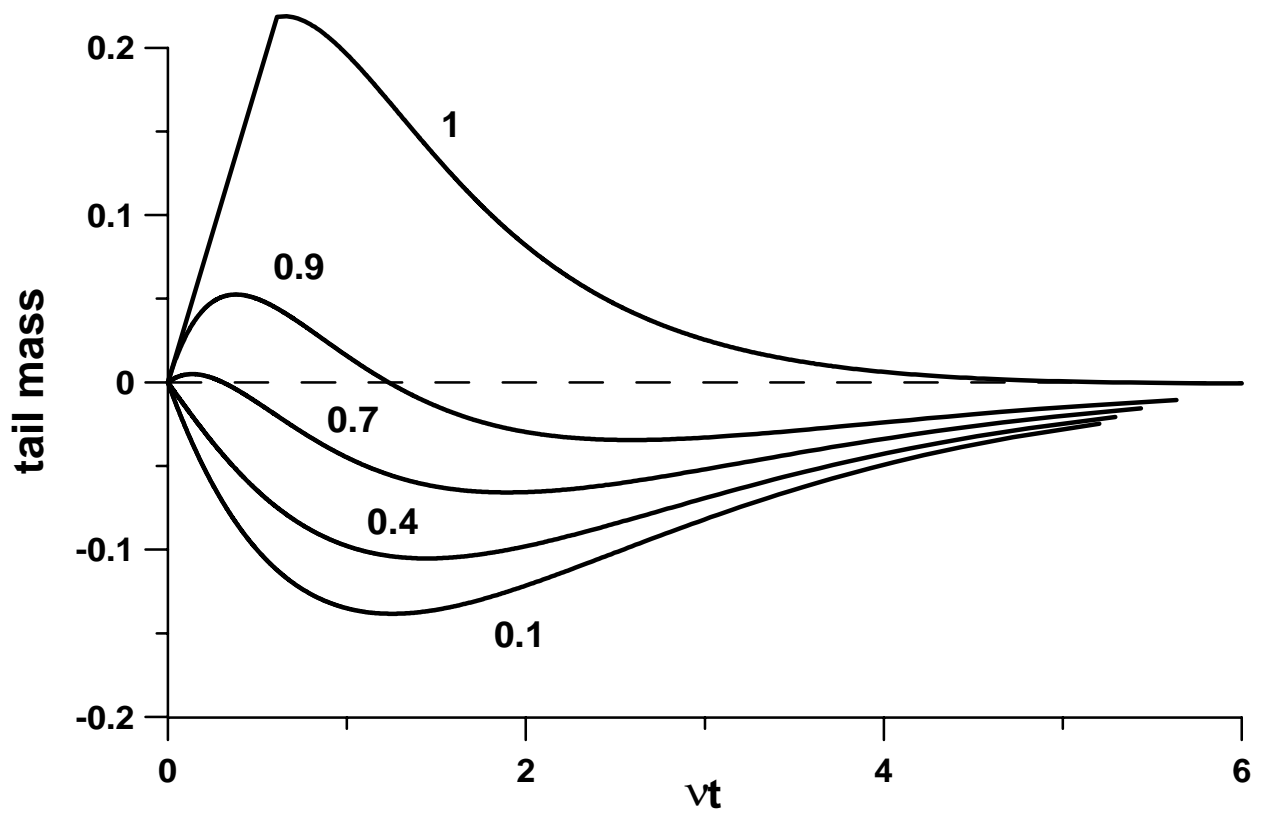


Figure 2. The tail mass as a function of time in the adiabatic approximation, for the linear friction case, when $\beta < 0$

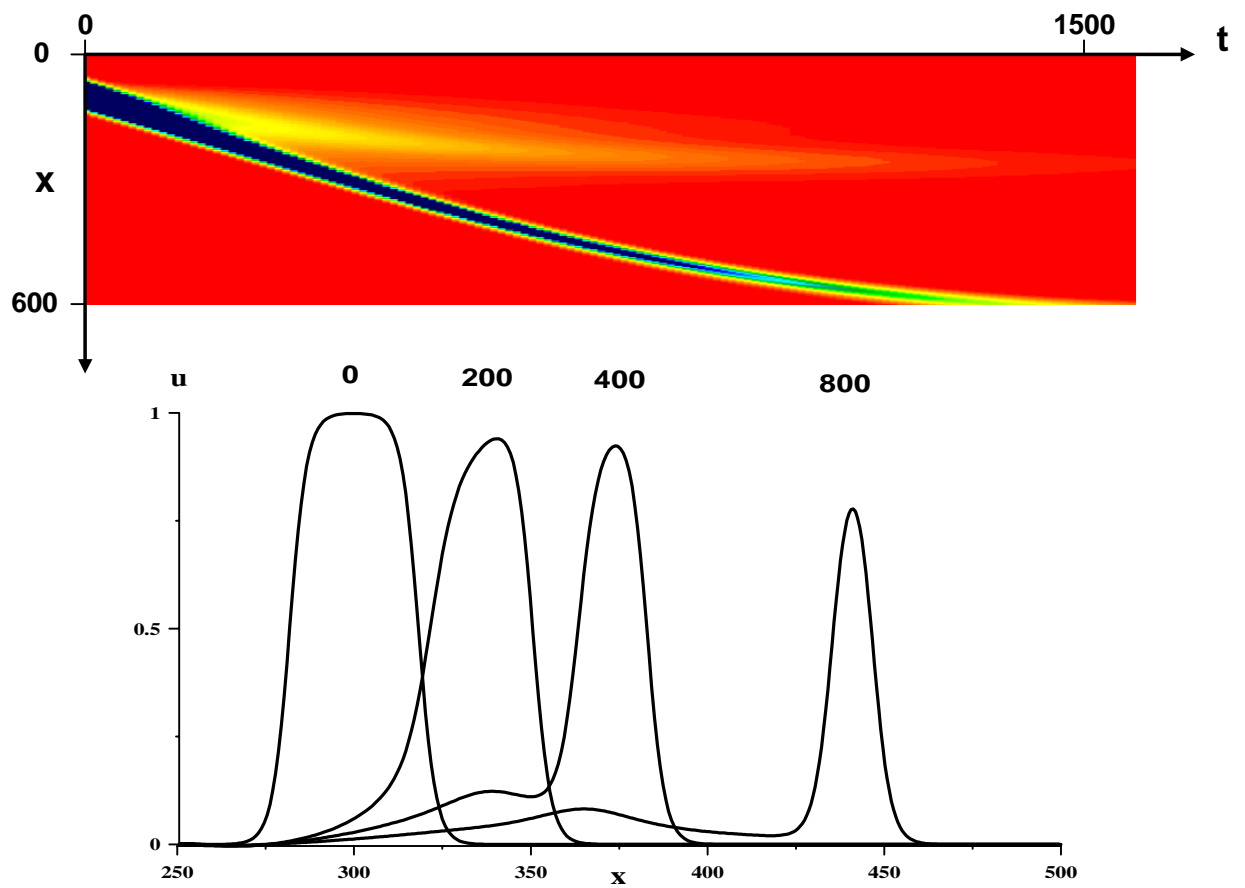


Figure 3. Evolution of the solitary wave for the linear friction case, $v = 0.001$, when $\beta < 0$

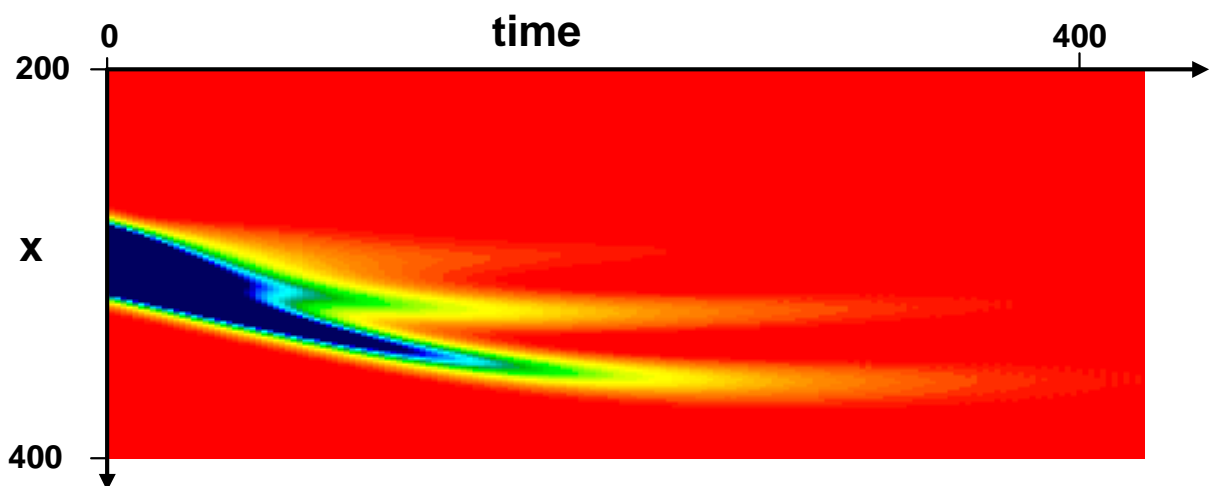


Figure 4. The same as in Figure 3, but for $v = 0.005$

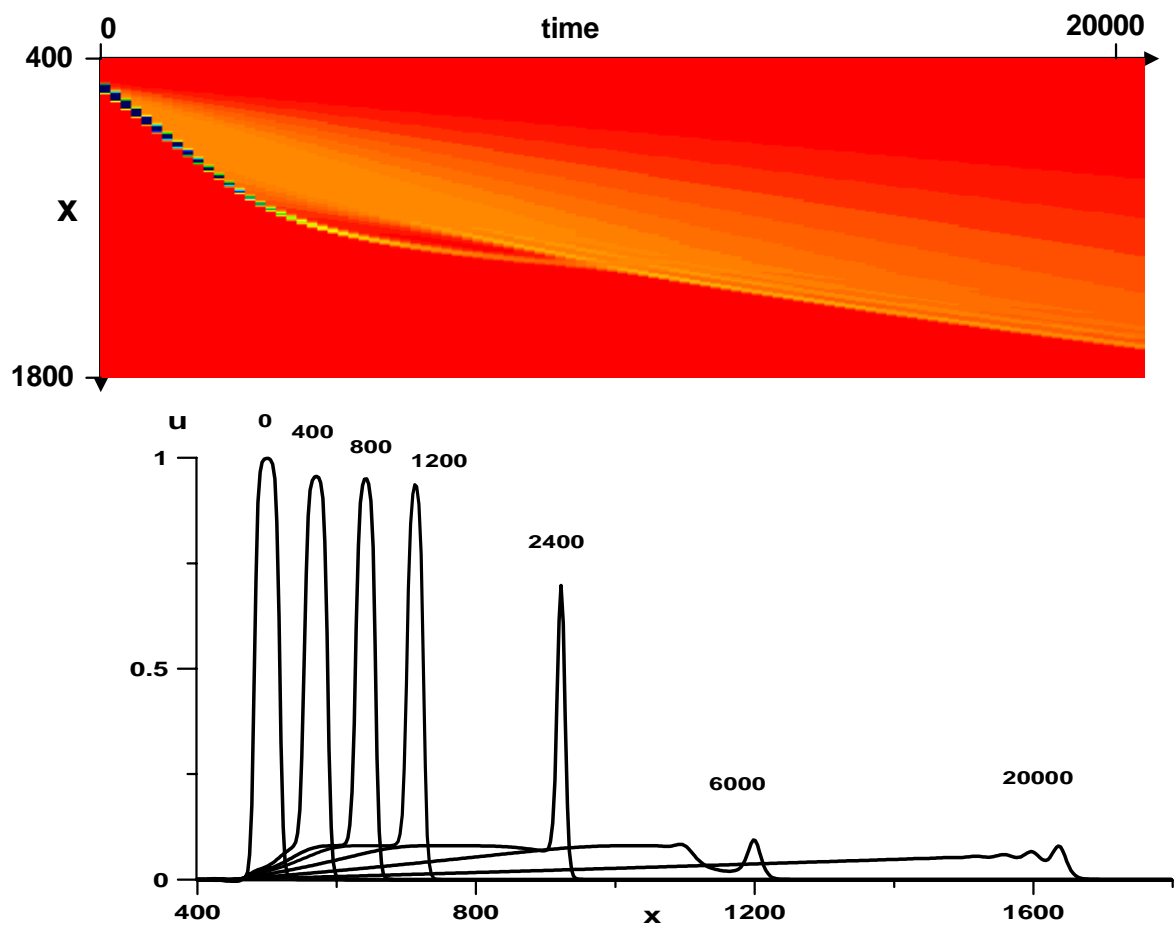


Figure 5. Evolution of the solitary wave for the linear viscosity case, $\nu = 0.05$, when $\beta < 0$

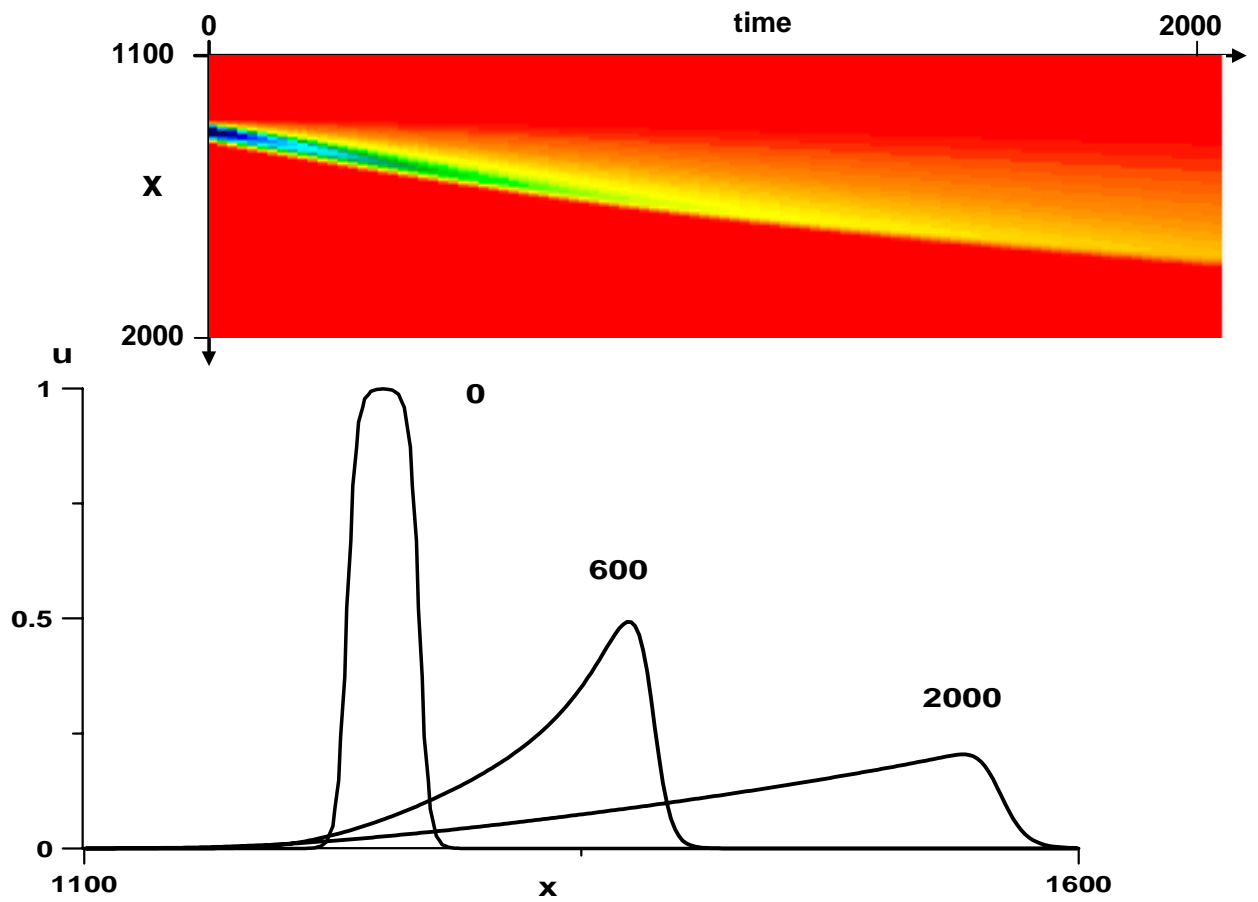


Figure 6. The same as in Figure 5, but for $\nu = 0.5$

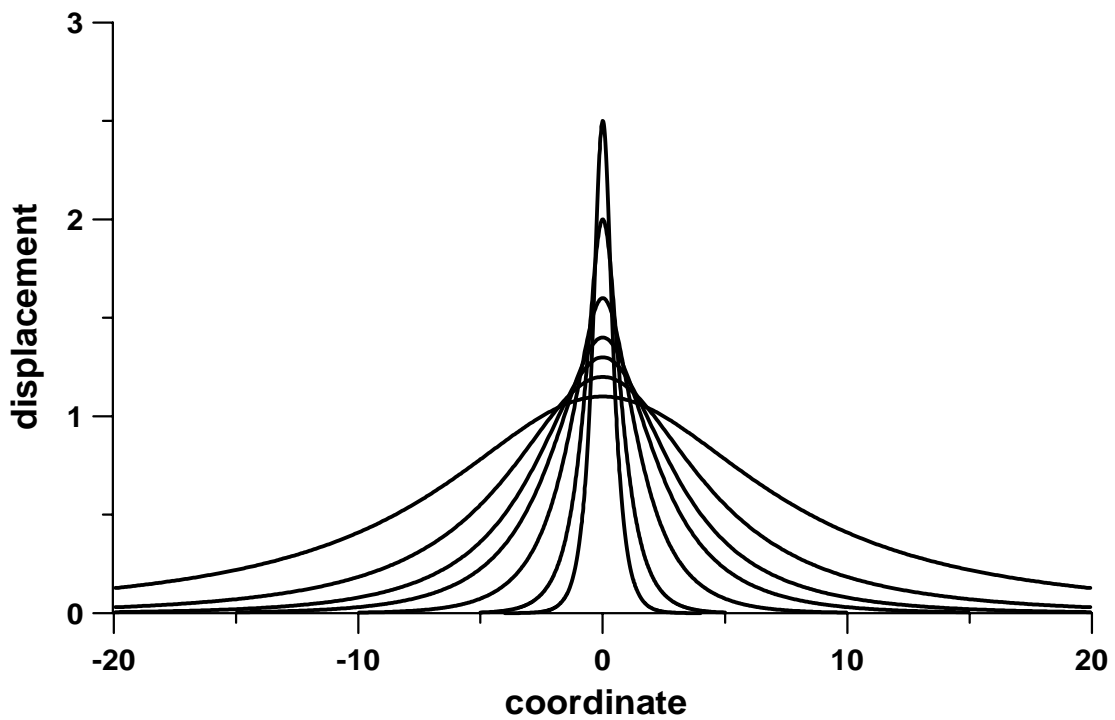


Figure 7. The shape of solitary wave solutions of equation (1) when the coefficient β of the cubic nonlinear term is positive

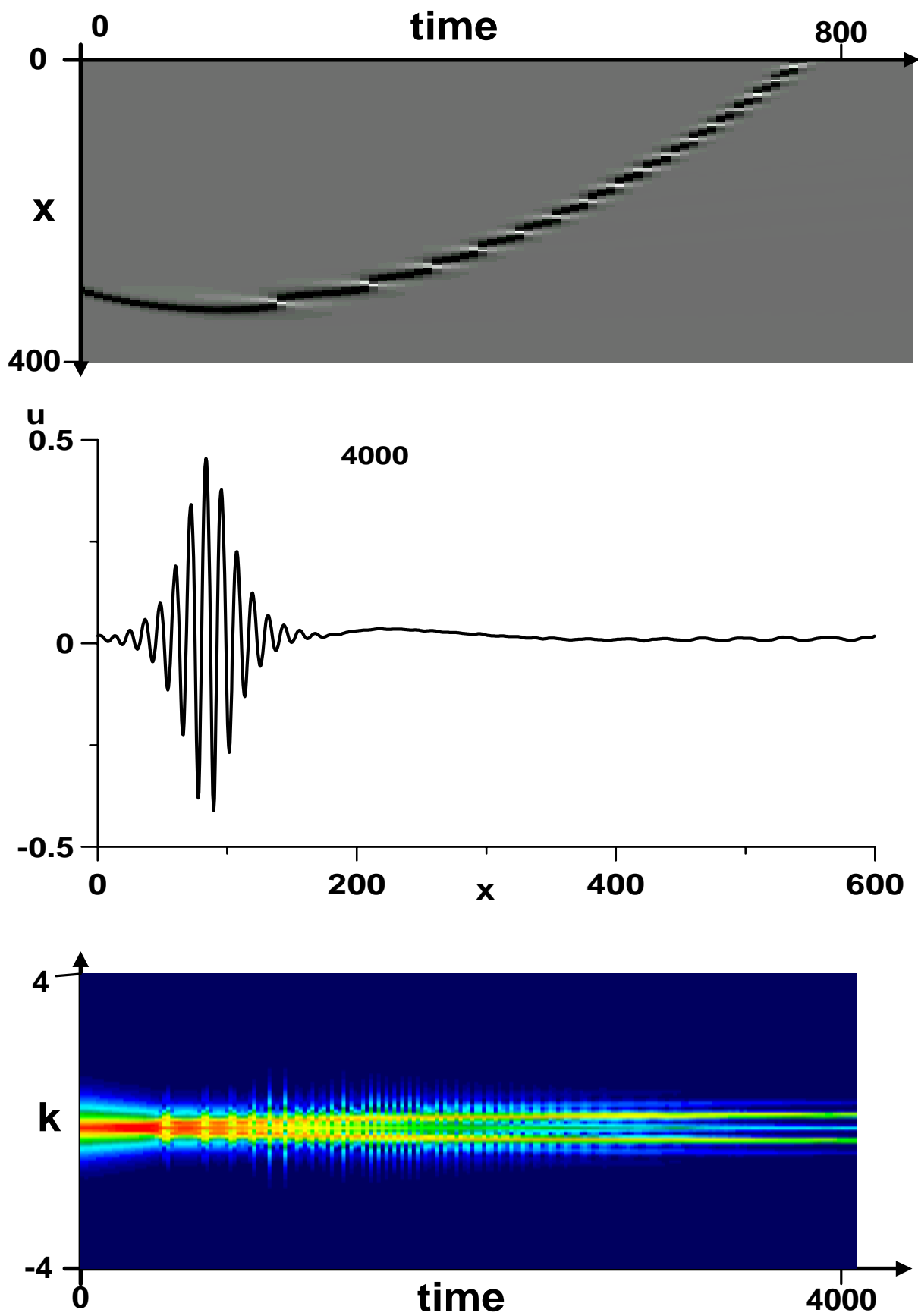


Figure 8. Transformation of a solitary wave into a wave packet for the linear viscosity case, $\nu = 0.001$, when $\beta > 0$.



Figure 9. The same as in Figure 8, but for $\nu = 0.015$

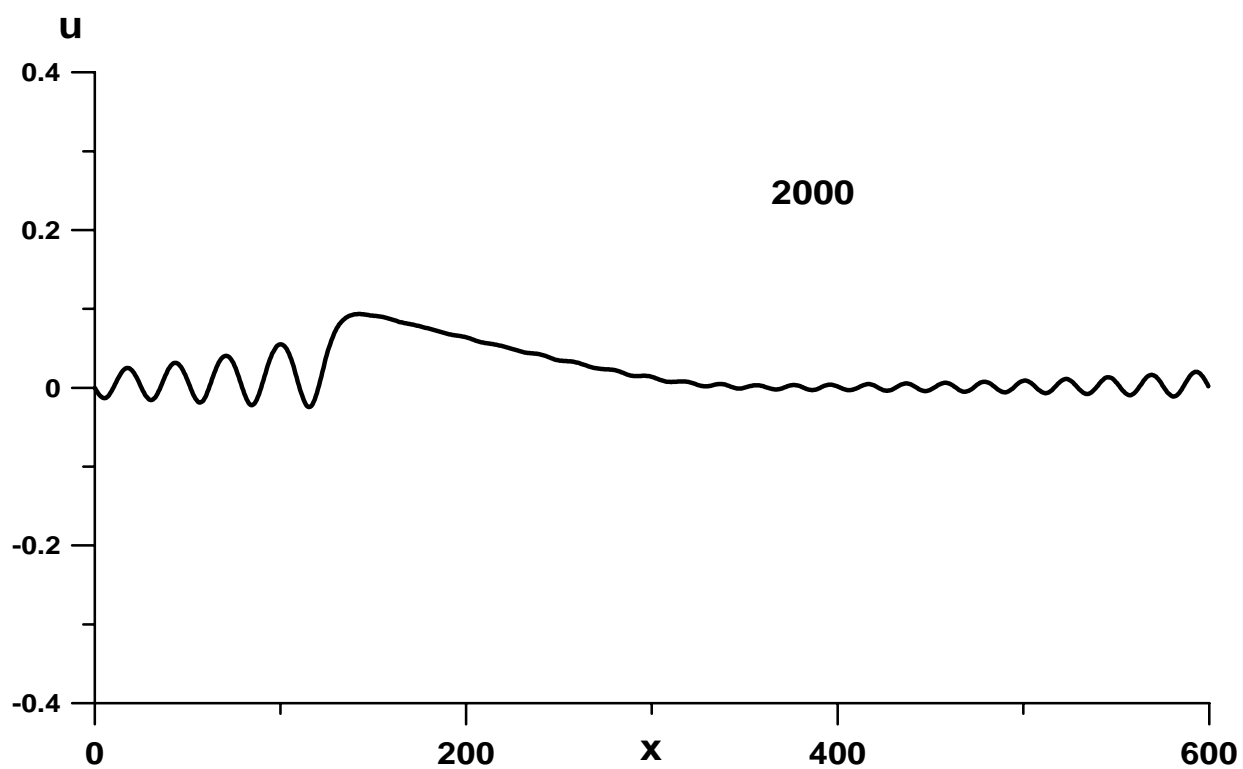
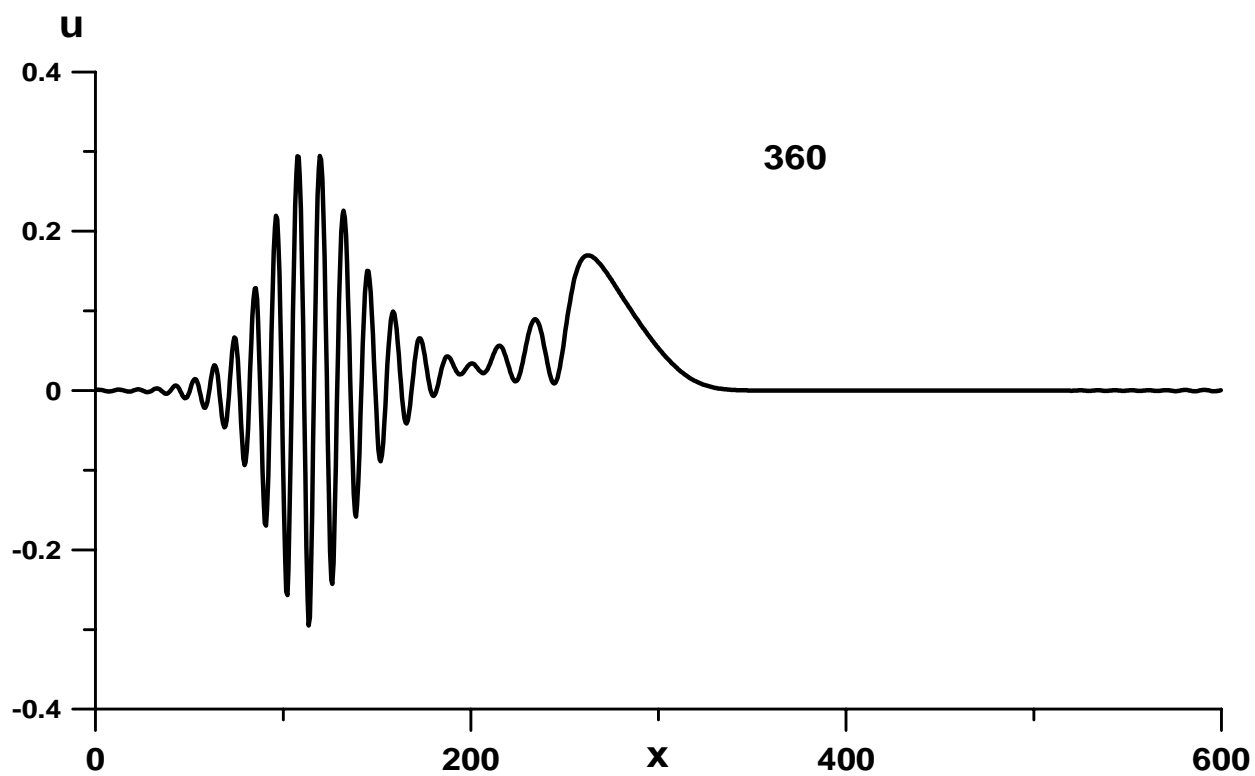


Figure 10. Long term evolution of the wave field after soliton damping, for the linear viscosity case, when $\beta > 0$

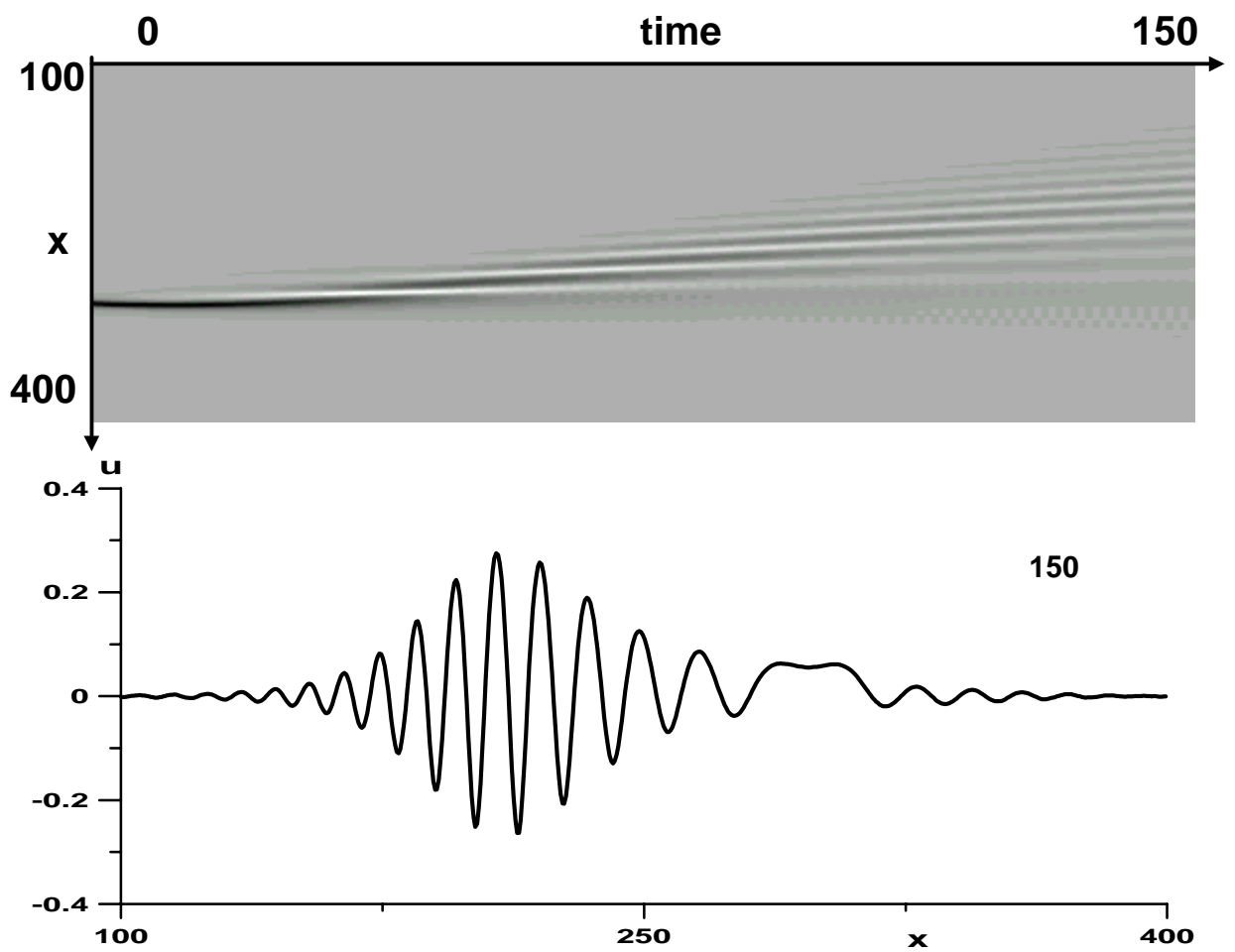


Figure 11. Transformation of a solitary wave into a breather for the linear friction case, when $\beta > 0$